Allosteric Effects of Nucleotide Cofactors on *Escherichia coli* Rep Helicase–DNA Binding

Isaac Wong and Timothy M. Lohman

The *Escherichia coli* Rep helicase unwinds duplex DNA during replication. The functional helicase appears to be a dimer that forms only on binding DNA. Both protomers of the dimer can bind either single-stranded or duplex DNA. Because binding and hydrolysis of adenosine triphosphate (ATP) are essential for helicase function, the energetics of DNA binding and DNA-induced Rep dimerization were studied quantitatively in the presence of the nucleotide cofactors adenosine diphosphate (ADP) and the nonhydrolyzable ATP analog AMPP(NH)P. Large allosteric effects of nucleotide cofactors on DNA binding to Rep were observed. Binding of ADP favored Rep dimers in which both protomers bound single-stranded DNA, whereas binding of AMPP(NH)P favored simultaneous binding of both single-stranded and duplex DNA to the Rep dimer. A rolling model for the active unwinding of duplex DNA by the dimeric Rep helicase is proposed that explains vectorial unwinding and predicts that helicase translocation along DNA is coupled to ATP binding, whereas ATP hydrolysis drives unwinding of multiple DNA base pairs for each catalytic event.

The transient unwinding of double-stranded (ds) DNA to form single-stranded (ss) DNA is an essential step in DNA replication, recombination, and repair and is catalyzed by DNA helicases in reactions that are coupled to the hydrolysis of nucleoside 5′-triphosphates (*1*, *2*). Helicases function at an unwinding fork [that is, the junction between duplex (ds) and ss-DNA] to unzip duplex DNA progressively by destabilizing the hydrogen bonds between the base pairs (bp). These enzymes occur in both prokaryotes and eukaryotes (*1–3*); 11 helicases have been identified in *Escherichia coli* alone (*4*, *5*). Helicases unwind duplex DNA in vitro in the absence of DNA synthesis, some at rates comparable to the rates of replication in prokaryotes (500 to 1000 bp per second). Some helicases that function in transcription (*6*), translation (*7*), and DNA repair (*8*, *9*) can unwind duplex RNA and RNA-DNA hybrids. Putative RNA helicases that may function in RNA splicing (*10*) have been identified on the basis of amino acid sequence comparisons (*11*).

The molecular details of the mechanism of DNA unwinding are not yet known for any helicase. In principle, a helicase could function by either a passive or active mechanism. In a passive mechanism, a helicase might bind to and translocate unidirectionally along only ss-DNA, catalyzing net DNA unwinding by binding to the ss-DNA that is formed transiently as a result of thermal fluctuations in the DNA duplex at an unwinding fork. Active mechanisms of DNA unwinding would require direct binding of the helicase to a region of the duplex DNA with subsequent destabilization of the duplex. Therefore a helicase that functions by an active mechanism might possess the ability to bind simultaneously to both ss- and ds-DNA (*5*). This requires the functional helicase to possess at least two DNA binding sites.

The *E. coli* Rep helicase is required for replication of a number of phages (for example, φX174, f1, and P2), and the rate of propagation of the *E. coli* chromosomal replication fork is reduced by a factor of ~2 in *rep* mutants (*12*). Although the *rep* gene is not essential in *E. coli* (*13*), *rep/uvrD* double mutants are lethal (*14*) as are some *rep/rho*(ts) double mutants (*15*); hence Rep may also be involved in DNA repair (*16*) and transcription (*15*).

Although the Rep protein is a monomer (72.8 kD) (*17*) up to concentrations of at least 8 μM, it forms a stable dimer on binding either ss- or ds-DNA, and chemically cross-linked Rep dimers retain both ss-DNA–dependent ATPase (adenosine 5′-triphosphatase) and DNA helicase activities (*18*, *19*). Each protomer of the Rep dimer can bind either ss- or ds-DNA, with both DNA conformations competing for the same site on each protomer, and dimers can bind ss- and ds-DNA simultaneously (*19*). The affinity of ss- or ds-DNA for a half-saturated Rep dimer is modulated by the conformation of the DNA that occupies the first site (*19*). These results suggest that the active form of Rep helicase is dimeric, thus providing the helicase with two DNA binding sites. In fact, the active forms of many helicases may be oligomeric in order to provide the helicase with multiple DNA binding sites (*5*).

The binding and hydrolysis of nucleoside 5′-triphosphate, usually ATP, is essential for helicase activity, and Rep appears to hydrolyze two molecules of ATP per base pair unwound (*20–22*). The binding and hydrolysis of ATP and the subsequent release of ADP (adenosine 5′-diphosphate) and inorganic phosphate may cause the helicase to cycle through a series of energy (conformational) states and may drive DNA unwinding vectorially (*5*, *21*, *23*). The unwinding process would then be propagated by repeated binding and hydrolysis of ATP and release of ADP. Such changes in conformational states induced by ATP and DNA binding have been observed for Rep (*24*).

In order to determine how a helicase functions, information about the energetics and dynamics of its interactions with both ss- and ds-DNA is needed, as both forms of DNA are present at an unwinding fork. However, for a multisite protein such as the DNA-induced Rep dimer, it is difficult to examine the effects if DNA binding at the separate sites of DNA molecules are long enough to bind simultaneously both Rep protomers. These complications can be circumvented with short oligodeoxynucleotides [16 nucleotides or base pairs] that preclude multiple binding of Rep monomers to a single oligonucleotide (*19*). Using these Rep dimer–oligodeoxynucleotide complexes to model intermediates that can form at an unwinding fork (Fig. 1), we determined the energetics of formation and the relative population distributions of these complexes in the presence and absence of the nucleotide cofactors ADP and the nonhydrolyzable ATP analog β-γ-imidoadenosine 5′-triphosphate [AMPP(NH)P].

Equilibrium constants for Rep DNA binding and dimerization. The equilibrium linkage scheme, the macroscopic equilibrium binding constants (K_{ijk}), and the Rep dimerization constants (L_{ijk}) (*25*) that de-

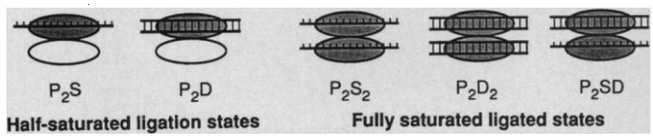

Fig. 1. Dimeric Rep–DNA complexes. Diagrammatic representation of the different Rep dimer–DNA species that can form in the presence of ss- and ds-oligodeoxynucleotides that are of sufficient length to allow only one Rep monomer to bind per oligodeoxynucleotide.

The authors are in the Department of Biochemistry and Molecular Biophysics, Washington University School of Medicine, 660 South Euclid Avenue, St. Louis, MO 63110.

scribe the interactions of Rep with short oligodeoxynucleotides (*19*) are shown in Fig. 2. A quantitative description of this system requires the determination of seven independent interaction constants, including five Rep DNA binding constants (K_{1S}, K_{2SS}, K_{1D}, K_{2DD}, and K_{2SD}) and two dimerization constants (L_{2S} and L_{2D}) (*19*). Because Rep monomers in the absence of DNA do not dimerize at concentrations up to at least 8 μM (*18*, *26*), we do not need to consider explicitly any equilibria involving the free Rep dimer at the low Rep concentrations (0.2 μM monomer) used in these studies. The remaining equilibrium constants (L_{2SS}, L_{2DD}, L_{2SD}, K_{2S}, and K_{2D}) can be calculated from the seven that are determined experimentally and an upper estimate of $L_2 \leq 10^4$ M^{-1} (*18*, *19*). All experiments were performed with $d(pT)_{16}$ as ss-DNA (*27*) and the 16-bp hairpin duplex oligodeoxynucleotide HP (5′-GACTCGTTACCTGAGT-T_4-ACTCAGGTTAACGAGTC) (*28*) as ds-DNA.

We obtained equilibrium isotherms for Rep-oligodeoxynucleotide binding using a double filter nitrocellulose filter binding method (*19*, *29*). To determine all seven interaction constants for each solution condition required three independent sets of filter binding experiments (*19*, *30*). In the first set, only $d(pT)_{16}$ was used to obtain the three constants K_{1S}, K_{2SS}, and L_{2S}, describing Rep interactions with ss-DNA (Fig. 2). In the second set, only the 16-bp HP was used to obtain the three constants K_{1D}, K_{2DD}, and L_{2D}, describing Rep–ds-DNA interactions (Fig. 2). For each case, two isotherms were measured, one at constant oligodeoxynucleotide concentration, varying the Rep concentration, and the other at constant Rep concentration, varying the DNA concentration (*19*, *30*). Finally, competition binding experiments performed in the presence of both $d(pT)_{16}$ and HP yielded K_{2SD} (*19*).

Effects of nucleotide cofactors on DNA binding and dimerization. In order to examine the effects of nucleotide cofactors on the equilibrium binding of ss- and ds-DNA to Rep, we performed titrations in the presence of either ADP (2 mM) or AMPP(NH)P (*31*), in buffer that contained 5 mM $MgCl_2$ (*30*). We compared three Rep-$d(pT)_{16}$ equilibrium binding isotherms obtained at constant Rep concentration in the presence of ADP(Mg^{2+}), AMPP(NH)P(Mg^{2+}), or Mg^{2+} alone (Fig. 3A). There was little qualitative effect of either nucleotide cofactor on the first phase of these isotherms, which reflects mainly monomer-DNA binding and dimerization (K_{1S} and L_{2S}); however, dramatic effects were observed on the second phase of the isotherms, indicating large changes in the relative affinities of $d(pT)_{16}$ for the unfilled subunit of the P_2S complex (K_{2SS}) (*32*).

Simultaneous nonlinear least-squares analysis of these isotherms in conjunction with isotherms obtained at constant $d(pT)_{16}$ concentration (*19*) yielded values of the three interaction constants K_{1S}, L_{2S}, and K_{2SS} for each condition (Table 1). The values of these constants showed that neither K_{1S} nor L_{2S} was sensitive to the binding of nucleotide cofactors. However, K_{2SS} decreased by more than a factor of 300 on replacing ADP(Mg^{2+}) with AMPP(NH)P(Mg^{2+}). Relative to the value of K_{2SS} in the absence of nucleotide, binding of AMPP(NH)P induced a decrease in K_{2SS}, whereas binding of ADP had the opposite effect. These effects were not the result of lowered free Mg^{2+} because of chelation by the nucleotide cofactors as indicated by independent experiments performed by varying the Mg^{2+} concentration (*33*).

The effects of nucleotide cofactors on the Rep–ds-DNA interaction constants

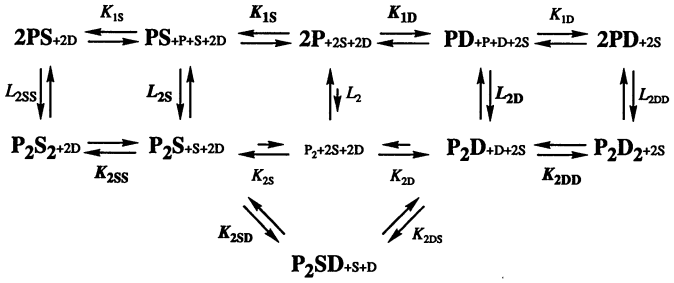

Fig. 2. Linkage scheme for DNA-induced Rep dimerization in the presence of both ss- and ds-oligonucleotides. The system is composed of eight protein species, namely, P, PS, PD, P_2S, P_2D, P_2S_2, P_2D_2, and P_2SD, where P, P_2, S, and D represent Rep monomer, Rep dimer, ss-DNA [$d(pT)_{16}$] and ds-DNA [16-bp hairpin (HP) duplex], respectively. The Rep-DNA binding constants are designated by the K_{ijk} and the Rep dimerization constants are designated by the L_{ijk} as defined in Table 1, where the first subscript, 1 or 2, designates whether the product formed is a Rep monomer or dimer, respectively, and the second and third subscripts, S or D, designate the species of DNA bound to Rep. The free Rep dimer, P_2, is not formed under the conditions of these experiments. Therefore only seven interaction constants are needed to fully describe this equilibrium scheme. The seven constants that we have chosen to use are indicated in bold.

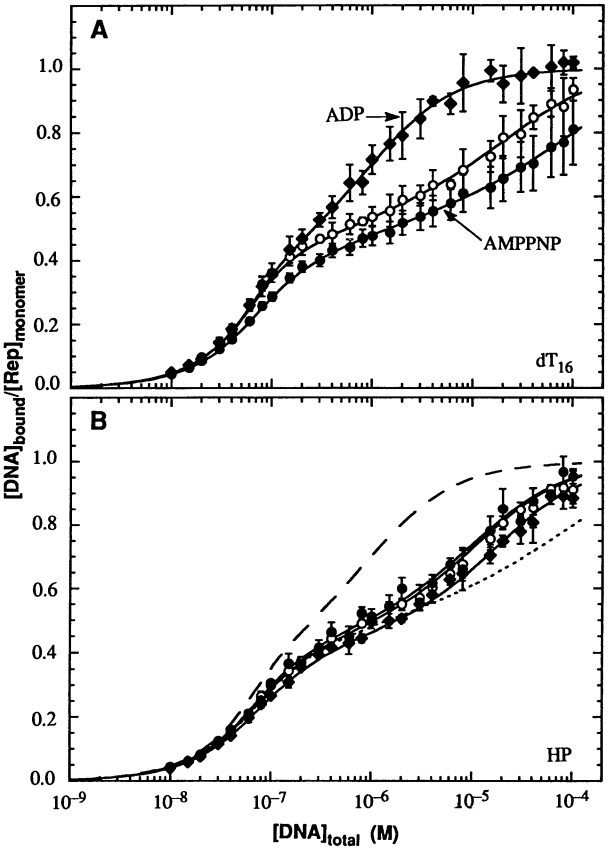

Fig. 3. Effects of nucleotide cofactors on Rep-DNA interactions. Nitrocellulose filter binding (*19*) was used to obtain equilibrium isotherms for Rep binding to (**A**) labeled ^{32}P-$d(pT)_{16}$ or (**B**) ^{32}P-HP ds-DNA at constant Rep concentration (0.2 μM of monomer) under standard conditions (20 mM tris, pH 7.5, 6 mM NaCl, 5 mM $MgCl_2$, 5 mM 2-mercaptoethanol, 10 percent (v/v) glycerol, 4°C) with no cofactor (open circles), 2 mM AMPP(NH)P (filled circles), or 2 mM ADP (filled diamonds). Rep was purified as described (*18*, *26*). Resolution of the three independent interaction constants, K_{1S}, L_{2S}, and K_{2SS} (or K_{1D}, L_{2D}, and K_{2DD}) was achieved by performing two equilibrium titrations for each solution condition, one at constant Rep concentration as shown and the other at constant DNA concentration (0.1 μM for dT_{16} and 0.2 μM for HP), followed by simultaneous nonlinear least-squares analysis of the two parallel titrations as described (*19*). Solid lines represent simulated isotherms obtained with the DNA-induced Rep dimerization model [Fig. 2, eq. 1 (*30*)] and the best-fit interaction constants in Table 1. For comparison, the simulated isotherms for Rep-dT_{16} binding from (A) in the presence of ADP (dashed) and AMPP(NH)P (dotted) are shown under the same conditions.

were examined with the 16-bp hairpin duplex HP (28). The Rep–ds-DNA isotherms were compared in the presence and absence of cofactors [2 mM ADP or AMPP(NH)P] (Fig. 3B). In each case, a 1:1 Rep monomer–HP stoichiometry was achieved at saturating DNA concentrations, an indication that both subunits of the Rep dimer can bind duplex DNA. These isotherms and the interaction constants determined from their analysis (Table 1) indicate that neither nucleotide cofactor significantly affected the Rep-HP equilibrium binding constants K_{1D} and K_{2DD}, although the dimerization constant L_{2D} was about three times greater in the presence of ADP(Mg^{2+}).

We further compared the Rep-HP duplex isotherms with those for Rep-d(pT)$_{16}$ (Fig. 3B). In 5 mM Mg^{2+} the isotherms for d(pT)$_{16}$ and HP binding to Rep were quite similar; however, in the presence of ADP or AMPP(NH)P these isotherms differed. The largest differences were observed in the second phase of the d(pT)$_{16}$ isotherms reflecting differences in the values of K_{2SS} for d(pT)$_{16}$ binding (32). In the presence of ADP, K_{2SS} was considerably larger than K_{2DD}, whereas the opposite was true in the presence of AMPP(NH)P (Table 1).

Modulation of competitive binding of ss- and ds-DNA to Rep by nucleotide cofactors. The HP duplex and d(pT)$_{16}$ bind competitively to the same sites on Rep monomers and dimers, and they can also bind simultaneously to a Rep dimer, one to each protomer, to form P_2SD (19). We therefore measured the effects of nucleotide cofactors on the competitive binding of d(pT)$_{16}$ and HP to Rep (Fig. 4, A to C). For each condition, two parallel experiments were performed in which a preformed Rep-d(pT)$_{16}$ complex was titrated with HP duplex. In one case, ^{32}P-labeled d(pT)$_{16}$ was used with unlabeled HP, whereas in the other case ^{32}P-labeled HP duplex was used with unlabeled d(pT)$_{16}$. In all experiments, the amount of Rep-bound ^{32}P-labeled DNA was monitored with nitrocellulose filter binding. In each condition, d(pT)$_{16}$ was completely displaced by the HP duplex. Furthermore, the stoichiometry of total DNA [d(pT)$_{16}$ and HP] bound never exceeded one per Rep monomer, indicating that ss- and ds-DNA compete for the same binding sites as shown in the absence of cofactors (19). However, the shape and symmetry of the competitive isotherms were affected by the presence of nucleotide cofactors, indicating quantitative differences in competitive binding and the ability to form P_2SD.

The competitive isotherms (Fig. 4, A to C) were analyzed to obtain K_{2SD}, the affinity of HP for the unfilled subunit of the P_2S dimer. We accomplished this by simulating a series of competition isotherms using Eqs. 3a and 3b (30). The six constants K_{1S}, K_{2SS}, L_{2S}, K_{1D}, K_{2DD}, and L_{2D} were constrained to their values in Table 1, having been determined independently, and the value of K_{2SD} was varied systematically until the simulated and experimental isotherms matched. The results (Table 1) indicated that K_{2SD} was lowest in the presence of only Mg^{2+}, increased ~5-fold in the presence of ADP(Mg^{2+}), and increased ~30-fold in the presence of AMPP(NH)P(Mg^{2+}).

The predicted population distributions for the saturated Rep dimer species P_2S_2, P_2D_2, and P_2SD in the presence of Mg^{2+}, ADP(Mg^{2+}), and AMPP(NH)P(Mg^{2+}) (Fig. 4, D to F) were calculated (19) with the use of the DNA-induced Rep dimerization model (Fig. 2) on the basis of the seven interaction constants in Table 1. Comparison of these distributions indicated that formation of P_2SD was favored in the presence of AMPP(NH)P(Mg^{2+}), whereas in the presence of ADP(Mg^{2+}), formation of P_2SD was suppressed and formation of P_2S_2 was favored. Neither P_2SD nor P_2S_2 was highly populated in the presence of only Mg^{2+}; under these conditions P_2S was dominant.

The affinity of either ss- or ds-DNA for the unfilled site of a half-saturated Rep dimer was modulated by the type of DNA bound to the first site (Table 1), indicating allosteric communication between the two DNA binding sites on Rep dimers (19). This behavior is apparent from comparisons of the intrinsic binding constants (25), k_{2XY}, which represent the binding of an oligodeoxynucleotide of conformation Y (Y = S or D) to a half-saturated Rep dimer P_2X (X = D or S). For example, the relative affinity of ds-DNA compared to ss-DNA for a Rep dimer with ss-DNA bound to one protomer (that is, P_2S) is given by $k_{2SD}/k_{2SS} = K_{2SD}/2K_{2SS}$ (25), and has a value of 0.043 under standard conditions (6 mM NaCl, pH 7.5, 4°C) in the absence of Mg^{2+} (19), indicating a strong preference for binding ss-DNA over ds-DNA to the second Rep protomer when ss-DNA is bound to the first protomer.

These allosteric effects were also modulated by nucleotide cofactors (Table 2), as k_{2SD}/k_{2SS} had values of 0.072, ≥146, and 1.25 in the presence ADP(Mg^{2+}), AMPP(NH)P(Mg^{2+}), and Mg^{2+} alone, respectively. Therefore, k_{2SD}/k_{2SS} increased by a factor of 2×10^3 on replacing ADP(Mg^{2+}) with AMPP(NH)P(Mg^{2+}). Because k_{2SD}/k_{2SS} is equivalent to the equilibrium constant for the transition from P_2S_2 to P_2SD (when $S_f = D_f$; f = free), these values indicate that AMPP(NH)P binding shifts the equilibrium population of dimers to favor formation of P_2SD, whereas ADP binding shifts the equilibrium to favor P_2S_2. Nucleotide cofactor binding affects primarily the interaction constants K_{2SS}, K_{2SD}, and K_{2DS}. All Rep dimerization constants and the equilibrium constants K_{1S} and K_{1D} for ss- and ds-DNA binding to Rep monomers, as well as K_{2DD}, were relatively unaffected by ADP or AMPP(NH)P (Table 1).

A rolling model for Rep dimer–catalyzed DNA unwinding. The observations that DNA binding induces Rep dimerization and that a cross-linked Rep dimer retains both DNA-dependent ATPase and

Table 1. The modulating effect of cofactors on Rep-oligodeoxynucleotide equilibrium interaction constants. All titrations were performed with the use of nitrocellulose filter binding (19, 29, 30) in 20 mM tris-HCl, pH 7.5, 4°C, 6 mM NaCl, 5 mM 2-mercaptoethanol, 10 percent glycerol, and 5 mM $MgCl_2$, with 2 mM AMPP(NH)P or ADP as indicated. The dT_{16} was used as ss-DNA (S) and a 16-bp duplex hairpin (HP) as ds-DNA (D). $K_{2DS} = K_{1S}L_{2S}K_{2SD}/K_{1D}L_{2D}$; $L_{2SS} = L_{2S}K_{2SS}/K_{1S}$; $L_{2DD} = L_{2D}K_{2DD}/K_{1D}$; $L_{2SD} = L_{2S}K_{2SD}/K_{1D}$; $K_{2S} = K_{1S}L_{2S}/L_2$; $K_{2D} = K_{1D}L_{2D}/L_2$. Upper estimate for L_2 is based on the observation that Rep in the absence of DNA is monomeric at concentrations up to 8 μM (18).

Reaction	Equilibrium constant ± SD* (μM^{-1})		
	$MgCl_2$	Mg · AMPP(NH)P	Mg · ADP
P + S ⇄ PS (K_{1S})†	2.1 ± 0.3	0.74 ± 0.12	2.5 ± 0.7
PS + P ⇄ P_2S (L_{2S})	200 ± 40	205 ± 30	190 ± 70
P_2S + S ⇄ P_2S_2 (K_{2SS})	0.0092 ± 0.0011	≤0.0025	0.83 ± 0.09
P_2S + D ⇄ P_2SD (K_{2SD})	0.023 ± 0.003	0.73 ± 0.08	0.12 ± 0.03
P + D ⇄ PD (K_{1D})	0.58 ± 0.13	0.80 ± 0.22	0.30 ± 0.14
PD + P ⇄ P_2D (L_{2D})	290 ± 70	240 ± 80	760 ± 150
P_2D + D ⇄ P_2D_2 (K_{2DD})	0.067 ± 0.008	0.066 ± 0.014	0.046 ± 0.007
P_2D + S ⇄ P_2SD (K_{2DS})	0.057	0.58	0.25
PS +PS ⇄ P_2S_2 (L_{2SS})	0.88	≤0.69	63
PD +PD ⇄ P_2D_2 (L_{2DD})	33.5	19.8	120
PS +PD ⇄ P_2SD (L_{2SD})	7.0	190	76
P_2 + S ⇄ P_2S (K_{2S})	≥4.2 × 10^4	≥1.5 × 10^4	≥4.8 × 10^4
P_2 + D ⇄ P_2D (K_{2D})	≥1.7 × 10^4	≥1.9 × 10^4	≥2.3 × 10^4
2P ⇄ P_2 (L_2)	≤0.01	≤0.01	≤0.01

*SD, standard deviation. †Symbol in parentheses is the equilibrium constant for the adjacent reaction.

DNA helicase activities suggest that the active form of the Rep helicase is dimeric (*18*). Therefore, the nucleotide cofactor–dependent modulation of the relative affinities of ss- and ds-DNA for the two sites on a Rep dimer is likely to be central to the mechanism of Rep-catalyzed DNA unwinding. Using the complexes formed between the DNA-induced Rep dimer and ss- and ds-oligodeoxynucleotides (Fig. 1) as models for Rep-DNA intermediates in DNA unwinding, we have shown the importance of two intermediates in the unwinding reaction (Table 2 and Fig. 4). On binding AMPP(NH)P, a P_2SD complex is formed in which ss- and ds-DNA are bound simultaneously to the Rep dimer, one to each protomer, whereas on binding ADP a P_2S_2 complex is formed in which both protomers of the Rep dimer are bound to ss-DNA.

On the basis of our observations we propose a model for the active unwinding of duplex DNA by the Rep helicase dimer (Fig. 5). We assume that ss-DNA binds each protomer with defined polarity with respect to its sugar-phosphate backbone and that like other dimeric proteins (*34*) the Rep dimer has C_2 symmetry (*34*). In the model, at least one subunit of the Rep dimer, although not always the same subunit, is bound to the 3′ ss-DNA at the fork, while the other subunit is bound either to the same single strand or to the adjacent duplex region ahead of the fork. Binding of ATP and its subsequent hydrolysis serve to modulate the affinities of the second Rep subunit so that binding to duplex DNA is favored when Rep is complexed with ATP(Mg^{2+}), whereas binding to ss-DNA is favored after hydrolysis of ATP to ADP.

In the model (Fig. 5) we start arbitrarily with a configuration (intermediate I) in which both Rep protomers are bound to the 3′ ss-DNA strand (corresponding to the leading strand in DNA synthesis), simulating a P_2S_2 complex (*35*). This configuration was chosen on the basis of the observation that initiation of DNA unwinding by the Rep helicase in vitro requires a 3′ ss-DNA flanking the duplex (*21*, *26*, *36*). On binding ATP, the affinity of the P_2S complex for ss-DNA in the second protomer decreases substantially (intermediate II) with a concomitant increase in the affinity of the P_2S complex for ds-DNA, resulting in the formation of intermediate III (P_2SD) in which the Rep dimer is bound simultaneously to the duplex ahead of the fork and the 3′ ss-DNA strand. In the next step (III to IV), hydrolysis of ATP by Rep induces conformational changes that unwind (denature) the region of duplex DNA bound to the Rep protomer, displacing the 5′ strand while remaining bound to the 3′ strand, thereby forming intermediate IV in which both protomers of the Rep dimer–ADP complex are bound to ss-DNA (P_2S_2). The subsequent release of ADP and inorganic phosphate leads to intermediate I′, which differs from intermediate I only in the relative positions of the individual subunits. However, because Rep is a homodimer, intermediates I and I′ are functionally equivalent, and the catalytic cycle is completed.

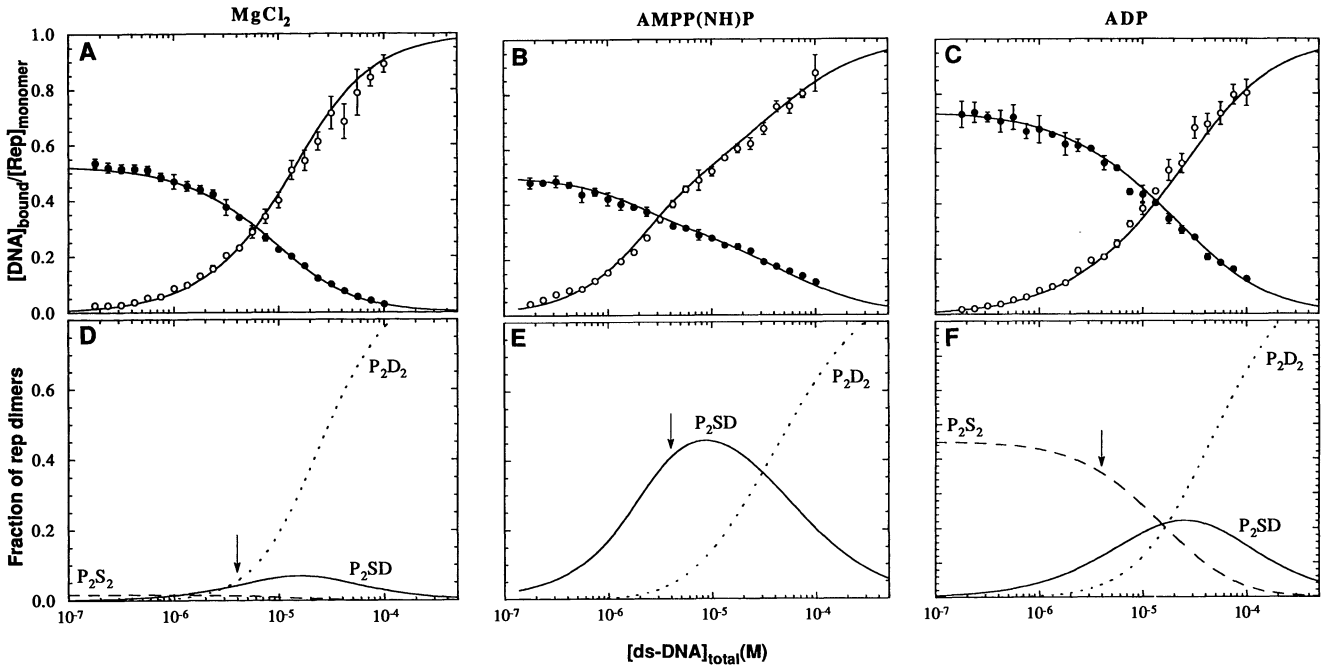

Fig. 4. Effects of cofactors on the competitive binding of ss- and ds-DNA to Rep. The competitive binding of ss- versus ds-oligodeoxynucleotides for Rep was examined with nitrocellulose filter binding (*19*). Preformed Rep-d$(pT)_{16}$ complexes (4 μM dT_{16} and 4 μM Rep monomer) were titrated with the 16-bp hairpin duplex, HP, under standard conditions (20 mM tris, pH 7.5, 6 mM NaCl, 5 mM $MgCl_2$, 5 mM 2-mercaptoethanol, 10 percent (v/v) glycerol, 4°C). Two parallel competition experiments were performed for each of the following conditions: (**A**) no cofactor, (**B**) 2 mM AMPP-(NH)P, and (**C**) 2 mM ADP. The ^{32}P-labeled dT_{16} (4 μM) (filled circles) was used, and the extent of ss-DNA binding to Rep was monitored as a function of added HP duplex. When the ^{32}P-labeled HP duplex was used (open circles), the amount of ds-oligodeoxynucleotide bound to Rep was monitored directly in the presence of unlabeled dT_{16} (4 μM). The competition curves were analyzed with the DNA-induced Rep dimerization model [Fig. 2; equations 3a and 3b (*30*)], and the best-fit values of K_{2SD} were obtained by varying K_{2SD} while constraining the six interaction constants K_{1S}, L_{2S}, K_{2SS}, K_{1D}, L_{2D}, and K_{2DD} to the values in Table 1. These six constants could be constrained, as their values had been determined from separate analyses of independent binding experiments with ss-DNA (dT_{16}) and ds-DNA (HP). The solid lines represent simulated isotherms generated with the DNA-induced Rep dimerization model [equations 3a and 3b (*30*)] and the seven interaction constants listed in Table 1 for each condition. In all cases, saturation with ds-DNA required complete dissociation of bound ss-DNA, indicating competitive binding to the same sites on the Rep dimer. The predicted population distributions of the doubly ligated Rep dimer species are shown in (**D**) no cofactor, (**E**) AMPP(NH)P, and (**F**) ADP. The fraction of Rep protein monomers present in each of the three doubly ligated states, P_2S_2 (dashed line), P_2D_2 (dotted line), and P_2SD (solid line), were calculated as a function of ds-DNA concentration under the conditions of the competition titrations with the DNA-induced Rep dimerization model (Fig. 2) and the equilibrium interaction constants in Table 1 as described (*19*). Arrows indicate the position at which the concentrations of ds-DNA, ss-DNA, and Rep monomer are equal (4 μM).

This model suggests that the Rep dimer rolls along the DNA, with translocation (steps I to III) coupled to ATP binding, and DNA unwinding (steps III to IV) coupled to ATP hydrolysis. Furthermore, each protomer of the Rep dimer does not remain bound to the DNA at all times during the unwinding process; rather, each subunit alternates among three states, namely, bound to ss-DNA, bound to duplex DNA, or dissociated from DNA. However, the functional helicase dimer always remains bound to the 3′ ss-DNA through at least one protomer. This model is therefore distinct from those that invoke sliding of the helicase along the DNA (that is, movement of a protomer along the DNA while the same protomer maintains continuous contact with the same DNA strand).

Our model predicts that translocation occurs in steps that are comparable to the site size of the protein (~16 nucleotides for Rep), rather than one nucleotide at a time, and that multiple base pairs are unwound per catalytic event (ATP hydrolysis). Although this appears to be in conflict with the observation that two molecules of ATP are hydrolyzed per base pair unwound during the Rep-catalyzed unwinding of duplex DNA (*20–22*), it is not likely that coupling of ATP hydrolysis to DNA unwinding is 100 percent efficient. In fact, a lower coupling efficiency (two ATP molecules hydrolyzed per bp unwound) could result from the mechanism in Fig. 5, as some uncoupled ATP hydrolysis should occur continuously because at least one Rep protomer is always bound to ss-DNA, and Rep–ss-DNA complexes have high ATPase activity. Therefore, it is possible that multiple base pairs are unwound per ATP hydrolyzed, but that this stoichiometry is not reflected directly in macroscopic measurements of ATP hydrolysis.

It has been generally assumed that helicases hydrolyze ATP in order to translocate unidirectionally along ss-DNA. However, the rolling model (Fig. 5) suggests that Rep dimer translocation along ss-DNA alone occurs by a random-walk mechanism without directional bias, as equivalent regions of ss-DNA exist on either side of the bound Rep dimer. In contrast, a net directional movement occurs during duplex DNA unwinding as a result of the presence of a duplex region that is covalently linked to the 5′ end of the ss-DNA. At an unwinding fork, the unliganded Rep protomer (Fig. 5, intermediate II) has two non-equivalent options for its next binding step because it is flanked on one side by ss-DNA and on the other side by ds-DNA. At equilibrium, the unbound Rep protomer in intermediate II binds to the DNA conformation for which it possesses the highest affinity, which is ds-DNA when Rep is bound with ATP; hence net directional transfer toward the duplex results from the presence and relative position of the duplex DNA and the influence of nucleotide cofactors on ss- versus ds-DNA binding. On the basis of the assumption that ss-DNA binds with a specific polarity to a Rep protomer, a Rep dimer would be unable to form the same type of P_2SD complex with a 5′ ss-DNA–duplex junction as it would with a 3′ ss-DNA–duplex junction. This suggests that Rep initiates unwinding only at one of these junctions as a result of its inability to form a correct initiation complex at the other junction, rather than as a result of unidirectional translocation along ss-DNA.

A helicase that functions by such a rolling mechanism should remain bound continuously to the DNA by at least one protomer. This provides a mechanism for the helicase to unwind DNA processively, although kinetic considerations such as the rate of Rep–ss-DNA dissociation and the efficiency of ATP hydrolysis influence the quantitative extent of processivity. The Rep helicase can unwind ϕX174 DNA (5386 bp) and fd phage DNA (~6000 bp) with high processivity in the absence of DNA synthesis after the supercoiled DNA has been nicked by the ϕX174 gene A or the fd gene II proteins, respectively (*21, 37*), thus providing the site for initiation of Rep helicase action.

Although DNA binding studies similar to those reported here are not yet available for other helicases, there are similarities between Rep and other helicases that suggest that some of the behavior observed for Rep may be general (5). Oligomeric assembly states, usually dimeric or hexameric, have been observed for all helicases examined, with the apparent exception of PriA (*38*). Examples include hexamers such as *E. coli* DnaB (*39*), SV40 large T antigen (*40*), and *E. coli* Rho (*41*) and dimers such as *E. coli* helicase III (*42*), phage T7 gene 4 protein (*43*), a human (HeLa) helicase (*44*), and the HSV-1 origin binding protein (*45*). The RecBCD protein, a recombinational helicase (*46*), forms at least a heterotrimer and possibly a hexamer [$(RecBCD)_2$] (*47*). Helicase II (*uvrD*) from *E. coli* (*48*) and the phage T4 gene 41 protein (*49*) also oligomerize. Like Rep, the *E. coli* DnaB protein can bind ss- and ds-DNA simultaneously (*50*), although the effects of nucleotide cofactors on the relative affinities of the individual DnaB subunits for ss- versus ds-DNA have not been determined. Therefore, it is possible that the active forms of many helicases are oligomeric, thus providing a means by which these enzymes acquire multiple DNA binding sites for use in mechanisms such as the one proposed in this article.

Table 2. Cofactor modulation of $P_2S_2 \rightleftarrows P_2SD$ equilibrium. $k_{2SD}/k_{2SS} = K_{2SD}/2K_{2SS}$. Values of K_{2SD} and K_{2SS} are taken from Table 1. $\Delta G° = -RT\ln(k_{2SD}/k_{2SS})$.

Cofactor	k_{2SD}/k_{2SS}	$\Delta G°$* (kcal/mol)	Preferred ligation state
Mg · ADP	0.072	+1.4	P_2S_2
Mg · AMPP(NH)P	≥146	≤−2.7	P_2SD
$MgCl_2$	1.25	−0.13	P_2S_2 + P_2SD

*Free energy change for the transition from P_2S_2 to P_2SD at 4°C assuming $S_f = D_f$ as would be the case for Rep bound at the unwinding fork.

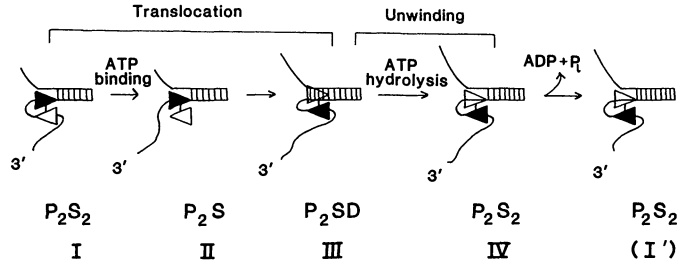

Fig. 5. Rolling model for Rep-catalyzed unwinding of duplex DNA. The dimeric Rep helicase is shown with triangular subunits assumed to be related by C_2 symmetry. The two Rep protomers are differentiated (filled versus unfilled) to indicate how the positioning of each protomer changes during the unwinding cycle.

REFERENCES AND NOTES

1. K. Geider and H. Hoffmann-Berling, *Annu. Rev. Biochem.* **50**, 233 (1981).
2. S. W. Matson and K. A. Kaiser-Rogers, *ibid.* **59**, 289 (1990).
3. P. Thommes and U. Hubscher, *FEBS Lett.* **268**, 325 (1990).
4. S. W. Matson, *Prog. Nucleic Acid Res.* **40**, 289 (1991).
5. T. M. Lohman, *Mol. Microbiol.* **6**, 5 (1992).
6. E. J. Steinmetz, C. A. Brennan, T. Platt, *J. Biol. Chem.* **265**, 18408 (1990).
7. B. K. Ray *et al.*, *ibid.* **260**, 7651 (1985).
8. S. W. Matson, *Proc. Natl. Acad. Sci. U.S.A.* **86**, 4430 (1989).
9. V. Bailly, P. Sung, L. Prakash, S. Prakash, *ibid.* **88**, 9712 (1991).
10. M. Company, J. Arena, J. Abelson, *Nature* **349**, 487 (1991); B. Schwer and C. Guthrie, *ibid.*, p. 494.
11. T. C. Hodgman, *ibid.* **333**, 22 (1988); D. Lane, *ibid.* **334**, 478 (1988).
12. H. E. D. Lane and D. T. Denhardt, *J. Bacteriol.* **120**, 805 (1974); *J. Mol. Biol.* **97**, 99 (1975).
13. J. Colasanti and D. T. Denhardt, *Mol. Gen. Genet.* **209**, 382 (1987).

14. B. K. Washburn and S. R. Kushner, *J. Bacteriol.* **173**, 2569 (1991).
15. J. S. Fassler, I. Tessman, E. S. Tessman, *ibid.* **161**, 609 (1985).
16. B. A. Bridges and A. von Wright, *Mutation Res.* **82**, 229 (1981).
17. C. A. Gilchrist and D. T. Denhardt, *Nucleic Acids Res.* **15**, 465 (1987).
18. K. Chao and T. M. Lohman, *J. Mol. Biol.* **221**, 1165 (1991).
19. I. Wong, K. Chao, W. Bujalowski, T. M. Lohman, *J. Biol. Chem.* **267**, 7596 (1992).
20. A. Kornberg, J. F. Scott, L. L. Bertsch, *ibid.* **253**, 3298 (1978).
21. G. T. Yarranton and M. L. Gefter, *Proc. Natl. Acad. Sci. U.S.A.* **76**, 1658 (1979).
22. N. Arai and A. Kornberg, *J. Biol. Chem.* **256**, 5294 (1981).
23. T. L. Hill and T. Tsuchiya, *Proc. Natl. Acad. Sci. U.S.A.* **78**, 4796 (1981).
24. K. Chao and T. M. Lohman, *J. Biol. Chem.* **265**, 1067 (1990).
25. The macroscopic equilibrium constants are designated with upper case symbols, K_{ijk} and L_{ijk}, whereas the intrinsic interaction constants are designated with lower case symbols, k_{ijk} and l_{ijk}. The first subscript refers to the final assembly state of the Rep protein (1 = monomer, 2 = dimer); the second and third subscripts indicate whether ss-DNA (S) or ds-DNA (D) is bound. The intrinsic constants have been corrected for statistical factors that are included in the macroscopic constants. The relation between the intrinsic and the macroscopic constants are (*19*): $k_{1S} = K_{1S}$; $k_{2S} = K_{2S}/2$; $k_{2SS} = 2K_{2SS}$; $l_2 = L_2$; $l_{2S} = L_{2S}/2$; $l_{2SS} = L_{2SS}$; $k_{1D} = K_{1D}/2$; $k_{2D} = K_{2D}/4$; $k_{2DD} = K_{2DD}$; $l_{2D} = L_{2D}/2$; $l_{2DD} = L_{2DD}$; $k_{2SD} = K_{2SD}$; $k_{2DS} = 2K_{2DS}$; $l_{2SD} = L_{2SD}$. Note that all of the macroscopic duplex DNA binding constants, K_{1D}, K_{2D}, K_{2DD}, and K_{2SD}, contain an additional statistical factor of 2, relative to the single-stranded macroscopic binding constants, on the basis of our assumption that a duplex DNA is likely to bind in two orientations, whereas ss-DNA is likely to bind in a unique orientation with respect to its backbone polarity.
26. T. M. Lohman, K. Chao, J. Green, S. Sage, G. Runyon, *J. Biol. Chem.* **264**, 10139 (1989).
27. Rep binding to ss-oligodeoxynucleotides does not display base composition dependence, hence Rep binding to $d(pT)_{16}$ reflects the general binding properties of Rep to ss-oligodeoxynucleotides of this length (*19*).
28. The equilibrium isotherm for Rep binding to the HP is identical to that of a 16-bp duplex dimer containing the identical duplex region under the conditions of these experiments (6 mM NaCl, pH 7.5, 4°C). Therefore, the 4-nucleotide T-loop in the hairpin does not influence the Rep-HP equilibrium interaction (*19*).
29. A modification of the nitrocellulose filter–binding method [A. Riggs *et al.*, *J. Mol. Biol.* **48**, 67 (1970)] was used to obtain equilibrium binding isotherms for the interactions of Rep with a series of ss- and ds-oligodeoxynucleotides (*19*). In this double-filter procedure, a 96-well dot-blot apparatus was used with sheets of nitrocellulose (Schleicher & Schuell) and DEAE paper (NA45, Schleicher & Schuell), with the nitrocellulose on top. Each Rep-DNA sample, representing one point in a titration, was loaded into one well of the 96-well apparatus. The nitrocellulose retains the Rep-bound ^{32}P-labeled DNA, and the DEAE filter retains the free ^{32}P-labeled DNA. The radioactivity retained within each dot on each filter sheet was quantitated by direct detection with a Betascope 603 Blot Analyzer (Betagen, Waltham, MA). With this approach, an entire binding isotherm consisting of a duplicate or triplicate set of 20 to 24 concentration points can be obtained on a single filter. Before use, nitrocellulose membranes were soaked for 10 minutes in 0.4 M KOH and then continuously rinsed in Milli-Q H_2O until the pH returned to neutral. Filters were then equilibrated in standard titration binding buffer at 4°C for a minimum of 1 hour before use. All samples for nitrocellulose filter binding were prepared in standard buffer (20 mM tris, pH 7.5, 6 mM NaCl, 5 mM $MgCl_2$, 1 mM EDTA, 5 mM 2-mercaptoethanol, 10 percent glycerol) at 4°C. Samples were mixed by repeated pipetting and then incubated at 4°C for 10 min. All samples were maintained at 4°C throughout the titration.
30. The extents of ss-DNA (S) and ds-DNA (D) binding are expressed either as the number of moles of oligodeoxynucleotide bound (b) per total (T) Rep monomer (S_b/P_T or D_b/P_T) or the fraction of total oligodeoxynucleotide bound (S_b/S_T or D_b/D_T), depending on whether the protein or DNA, respectively, is held constant in the titration. For the binding of ss-DNA to Rep in the absence of duplex DNA, the expressions for these quantities in terms of the DNA-induced Rep dimerization model (Fig. 2) (*19*) are given in Eqs. 1 and 2,

$$S_b/P_T = K_{1S}S_f[1 + L_{2S}P_f(1 + 2K_{2SS}S_f)] \div (1 + K_{1S}S_f[1 + 2L_{2S}P_f(1 + K_{2SS}S_f)]) \quad (1)$$

$$S_b/S_T = K_{1S}P_f[1 + L_{2S}P_f(1 + 2K_{2SS}S_f)] \div (1 + K_{1S}P_f[1 + L_{2S}P_f(1 + 2K_{2SS}S_f)]) \quad (2)$$

where S, D, and P refer to ss-DNA, ds-DNA, and Rep monomer, respectively, and the subscripts b, f, and T refer to bound, free, and total, respectively. Expressions for D_b/P_T and D_b/D_T can be obtained from eqs. 1 and 2 by replacing K_{1S}, L_{2S}, K_{2SS}, and S_f with K_{1D}, L_{2D}, K_{2DD}, and D_f, respectively. The mixed ligation state Rep dimer, P_2SD, in which ss-DNA and ds-DNA are bound simultaneously to the Rep dimer, can be formed in the presence of both ss- and ds-oligodeoxynucleotides. P_2SD can be formed either by binding of S to P_2D with binding constant K_{2DS} or by binding of D to P_2S with binding constant K_{2SD}; however, only one of these binding constants is needed to define the equilibria involving P_2SD. All seven independent equilibrium constants (K_{1S}, L_{2S}, K_{2SS}, K_{1D}, L_{2D}, K_{2DD}, and K_{2SD}) are needed to describe the competitive binding of ss- and ds-oligodeoxynucleotides to Rep, and the expressions for S_b/P_T and D_b/P_T in the presence of both S and D are given in Eq. 3, a and b (*19*).

$$S_b/P_T = K_{1S}S_f[1 + L_{2S}P_f(1 + 2K_{2SS}S_f + K_{2SD}D_f)] \div (1 + K_{1S}S_f + K_{1D}D_f + 2P_f[K_{1S}L_{2S}S_f (1 + K_{2SS}S_f + K_{2SD}D_f) + K_{1D}L_{2D}D_f(1 + K_{2DD}D_f)]) \quad (3a)$$

$$D_b/P_T = K_{1D}D_f[1 + L_{2D}P_f(1 + 2K_{2DD}D_f)] + (K_{1S}L_{2S}K_{2SD}P_fS_fD_f) \div (1 + K_{1S}S_f + K_{1D}D_f + 2P_f[K_{1S}L_{2S}S_f (1 + K_{2SS}S_f + K_{2SD}D_f) + K_{1D}L_{2D}D_f(1 + K_{2DD}D_f)]) \quad (3b)$$

31. We found that ATP-γ-S is hydrolyzed slowly by Rep when bound to $d(pT)_{16}$, whereas AMPP-(NH)P is not hydrolyzed detectably under the conditions of these experiments.
32. The biphasic character of the isotherms [especially in the presence of AMPP(NH)P], with a plateau near 0.5 $d(pT)_{16}$ bound per Rep monomer [1 $d(pT)_{16}$ per Rep dimer], indicates the formation of a stable half-saturated intermediate state, P_2S (Fig. 1), under these conditions. The first phase reflects both the binding of $d(pT)_{16}$ to a Rep monomer to form a 1:1 complex, PS, followed by dimerization to form P_2S; hence this phase is sensitive to K_{1S} and L_{2S} (*19*). At higher $d(pT)_{16}$ concentrations, a second DNA molecule binds to the Rep dimer to form the fully saturated species P_2S_2; hence the second phase reflects mainly K_{2SS}.
33. Because chelation of Mg^{2+} by ADP and AMPP-(NH)P lowers the free Mg^{2+} concentration, we also examined the effects of $MgCl_2$ at concentrations of 1, 3, 5, and 25 mM. No effect of Mg^{2+} on the Rep dimerization constant L_{2S} was observed. The value of K_{1S} decreased by a factor of two on adding 1 mM $MgCl_2$, although no further change occurred between 1 to 5 mM $MgCl_2$. The largest effect of Mg^{2+} was on K_{2SS}, which decreased substantially on addition of 1 mM $MgCl_2$ (from 3.8×10^6 M^{-1} to 1.7×10^4 M^{-1}). However, the values of K_{2SS}, K_{1S}, and L_{2S}, did not change on increasing the $MgCl_2$ concentration from 1 to 5 mM.
34. C_2 symmetry reflects a twofold axis of symmetry [B. W. Matthews and S. A. Barnhardt, *Annu. Rev. Biophys. Bioeng.* **2**, 257 (1973)].
35. At the dT_{16} concentrations used, our binding data suggest that the preferred ligation state in the absence of cofactors is the half-saturated species P_2S, rather than the fully saturated P_2S_2. However, if the dT_{16} concentration is high enough, then P_2S_2 will form even in the presence of Mg^{2+} alone. Therefore, we have chosen to use P_2S_2 to represent intermediates I and I′, because at the replication fork the 3′ ss-DNA is a single piece of polymeric DNA; hence the local concentration of ss-DNA will be much higher than the dT_{16} in our experiments. This high local concentration should favor formation of P_2S_2 rather than P_2S. However, the actual ligation state of the Rep dimer in the absence of cofactor (states I and I′) is not important for the model. Any state could be substituted for state I or I′ (Fig. 5) without modification of the principal tenets of the model, which hinge on the influence of ADP compared to AMPP(NH)P on the relative affinity of ds- versus ss-DNA for the second site of the Rep dimer.
36. G. T. Runyon and T. M. Lohman, *J. Biol. Chem.* **264**, 17502 (1989).
37. S. Eisenberg, J. D. Griffith, A. Kornberg, *Proc. Natl. Acad. Sci. U.S.A.* **74**, 3198 (1977).
38. R. S. Lasken and A. Kornberg, *J. Biol. Chem.* **263**, 5512 (1988). The PriA protein appears to be a stable monomer in the absence of DNA. However, because the Rep protein only dimerizes when bound to DNA, the assembly state of PriA must be examined when bound to DNA before it can be concluded that it functions as a monomer.
39. L. J. Reha-Krantz and J. Hurwitz, *J. Biol. Chem.* **253**, 4043 (1978).
40. I. A. Mastrangelo *et al.*, *Nature* **338**, 658 (1989).
41. L. R. Finger and J. P. Richardson, *J. Mol. Biol.* **156**, 203 (1982).
42. G. T. Yarranton, R. H. Das, M. L. Gefter, *J. Biol. Chem.* **254**, 12002 (1979).
43. J. A. Bernstein and C. C. Richardson, *ibid.* **263**, 14891 (1988).
44. Y.-S. Seo, S.-H. Lee, J. Hurwitz, *ibid.* **266**, 13161 (1991).
45. R. C. Bruckner, J. J. Crute, M. S. Dodson, I. R. Lehman, *ibid., p. 2669.*
46. G. R. Smith, in *Nucleic Acids and Molecular Biology*, F. Eckstein and D. M. J. Lilley, Eds., (Springer-Verlag, Berlin, 1990), vol. 4, pp. 78–98.
47. C. C. Dykstra, K. M. Palas, S. R. Kushner, *Cold Spring Harbor Symp. Quant. Biol.* **49**, 463 (1984).
48. G. T. Runyon and T. M. Lohman, unpublished data.
49. C. C. Liu and B. Alberts, *J. Biol. Chem.* **256**, 2813 (1981).
50. K. I. Arai, N. Arai, A. Kornberg, *ibid., p. 5247.*

51. We thank W. Van Zante for help with oligodeoxynucleotide purification, K. Chao for preliminary experiments, and L. Lohman for help with the figures. Supported in part by NIH grants GM30498 and GM45948, American Cancer Society grant NP-756, American Cancer Society Faculty Research Award FRA-303 (T.M.L.), and an American Cancer Society Postdoctoral Fellowship (PF-3671) (I.W.).

6 December 1991; accepted 4 March 1992